*Journal of Inclusion Phenomena and Macrocyclic Chemistry* **45:** 19–25, 2003.



# Investigation of the Formation of Inclusion Complexes between Rhodamine 6G and Cyclodextrins by Means of Capillary Electrophoresis Using Poly(vinyl sulfate)

SANYO HAMAI* and KATSUMI SASAKI
*Department of Chemistry, Faculty of Education and Human Studies, Akita University, Tegata Gakuen-machi 1-1, Akita 010-8502, Japan*

(Received 11 December 2001; in final form: 22 October 2002)

*Key words:* cyclodextrins, Rhodamine 6G, poly(vinyl sulfate), inclusion complexes, capillary electrophoresis, spectrophotometry

**Abstract**

In capillary electrophoresis using poly(vinyl sulfate), added to sample solutions and running buffers, the signal of Rhodamine 6G (R6G) is shaped like a square wave. When $\alpha$-, $\beta$-, or $\gamma$-cyclodextrin ($\alpha$-, $\beta$-, or $\gamma$-CD) has further been added to the running buffers as well as sample solutions, the intensity of the square-wave type signal of R6G has been enhanced, accompanied by narrowing of the signal width. The migration time of the rising edge of the square-wave type signal has been very slightly delayed by the addition of CD. These findings exhibit the formation of inclusion complexes of R6G with CDs. From the analyses of the variations in signal width with the concentration of CD, the equilibrium constants for the formation of the 1:1 inclusion complexes of R6G with $\alpha$-, $\beta$-, and $\gamma$-CDs have been evaluated to be 245, 210, and 302 $M^{-1}$, respectively, although the equilibrium constants could not be estimated using a conventional procedure based on electrophoretic mobility, in which poly(vinyl sulfate) was not added. The values of the equilibrium constants for $\beta$- and $\gamma$-CDs are comparable to those obtained from the absorbance changes in spectrophotometry, whereas the value for $\alpha$-CD is about four times greater than that obtained from the absorbance change.

## Introduction

Commercially available cyclodextrins (CDs) are cyclic oligomers composed of six, seven, and eight D-glucopyranose residues, which are called $\alpha$-, $\beta$-, and $\gamma$-CD, respectively [1]. CDs are shaped like a truncated cone with a relatively hydrophobic cavity. The exterior of the CD cavity is hydrophilic due to many hydroxy groups perched on the narrow and wide CD rims. In aqueous solutions, therefore, a wide variety of organic compounds are incorporated into the CD cavity to form inclusion complexes. CDs have the potential of modifying chemical reactions and achieving molecular recognition, including chirality [2–11]. Consequently, the characteristic abilities of CDs have been focused upon and have been studied extensively.

Recently, we have investigated the interactions between Rhodamine 6G (R6G) and poly(vinyl sulfate) (PVS) by means of capillary electrophoresis, in which PVS has been added to sample solutions and running buffers [12]. Above a PVS concentration of around 3.0 mg $L^{-1}$, the signal of R6G in capillary electrophoresis is shaped like a square wave. As the R6G concentration is increased at a fixed concentration of PVS, the width of the square-wave type signal is increased, although the signal intensity remains constant; the migration time of the falling edge of the square-wave type signal is lengthened, whereas nearly the same migration time has been observed for the rising edge of the signal. When the PVS concentration is decreased at a fixed R6G concentration, the width of the square-wave type signal is reduced, accompanied by an increase in the signal intensity.

These results observed for the PVS-modified capillary electrophoresis, in which PVS has been added to samples and running buffers, have been explained in terms of the cooperative binding of R6G to PVS [12]. The signal behavior has been well reproduced by simulations based on a model where the binding constant of R6G towards PVS has either a large or a small value, depending on the concentration (number) of R6G molecules in a very small consecutive domain, into which the space inside a capillary tube is divided. The assumption in the simulations implies cooperative binding of R6G to PVS.

The evaluation of the equilibrium constants for the formation of inclusion complexes of CD with guest molecules by means of conventional capillary electrophoresis is based on the variation of the migration time (electrophoretic mobility) of a guest with the CD concentration [8, 13]. In some cases, however, a reliable value of the equilibrium constant cannot be evaluated, because the change in migration time is small upon the addition of CD. To perform accurate measurements of migration time shifts, there are

* Author for correspondence.

several procedures by which the effective length of a capillary is increased. Recently, a pressure-mediated capillary electrophoretic method has been proposed for the evaluation of weak binding constants [14]. Although these are superior methods, they are relatively tiresome and time-consuming.

Under our experimental conditions of capillary electrophoresis, the migration-time shifts of R6G were small upon the addition of CD. Thus, we have tried to employ PVS-modified capillary electrophoresis, in which PVS has been added to sample solutions and running buffers, to estimate the equilibrium constants for the formation of the inclusion complexes of R6G with CDs. In addition, the equilibrium constants thus obtained have been compared with those estimated from spectrophotometric analyses.

## Experimental

Rhodamine 6G (R6G) and poly(vinyl sulfate) (PVS), which were obtained as a chloride and a potassium salt from Tokyo Kasei Kogyo and nacalai tesque, respectively, were used as received. Although purified PVS, which was dialyzed using UC24-32-100 dialysis tubing (Viskase Sales) for one day, was used in several experiments, the same results as those for undialyzed PVS were obtained. $\beta$-Cyclodextrin ($\beta$-CD) purchased from nacalai tesque was twice recrystallized from water. $\alpha$-CD and $\gamma$-CD, obtained from nacalai tesque and Wako Pure Chemical, respectively, were used without further purification.

Aqueous buffers (pH 7.5) of $KH_2PO_4$ ($5.0 \times 10^{-4}$ M) $-$ $Na_2HPO_4$ ($2.0 \times 10^{-3}$ M) were employed for capillary electrophoresis and spectrophotometry. In capillary electrophoresis, PVS (100 mg $L^{-1}$) and/or CD were added to both sample solution and running buffer, except for the experiments without PVS and/or CD; the sample matrix was the same as the running buffer. The concentrations of R6G were $2.5 \times 10^{-4}$ and $1.0 \times 10^{-5}$ M for the measurements of capillary electrophoresis and spectrophotometry, respectively.

Capillary electrophoresis was performed using a Hitachi U-2000 spectrophotometer and a Matsusada Precision Device HCZE-30 PN apparatus as a detector and a high-voltage power supply, respectively. The detection wavelength was 525 nm for capillary electrophoresis. The applied voltage was maintained at 15.0 kV throughout this study. A GL Science uncoated fused-silica capillary (70.0 cm $\times$ 0.05 mm i.d.) was employed for the measurements of capillary electrophoresis. The effective length of the capillary tube was 30.0 cm (from the injection end to the detection window). Samples were gravity injected into the capillary for 30 s at 4.0 cm.

Absorption spectra were recorded on a Shimadzu UV-260 spectrophotometer.

In capillary electrophoresis and spectrophotometry, all of the measurements were made at 25 °C.

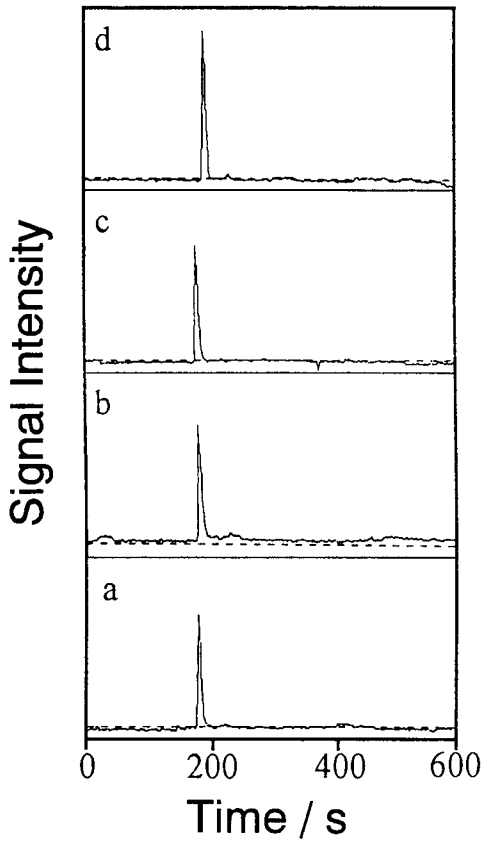


*Figure 1.* Electropherograms of R6G ($2.5 \times 10^{-4}$ M) in pH 7.5 buffers containing various concentrations of $\beta$-CD. Concentration of $\beta$-CD: (a) 0, (b) $1.0 \times 10^{-3}$, (c) $3.0 \times 10^{-3}$, and (d) $1.0 \times 10^{-2}$ M. The ordinate scales of the electropherograms are the same.

## Results and discussion

### *Capillary electrophoresis of R6G using running buffer without PVS*

Figure 1 shows electropherograms of R6G in pH 7.5 buffers, which do not contain PVS, in the absence and presence of $\beta$-CD. The migration time of R6G is slightly increased from 180 to 198 s, as the $\beta$-CD concentration is increased from 0 to $1.0 \times 10^{-2}$ M. Because an R6G molecule is a cation, the delay of the migration time of R6G indicates an increase in the effective bulkiness of R6G; the increase in the migration time is due to the formation of an inclusion complex of R6G with $\beta$-CD. Because the increase in the migration time by the addition of $\beta$-CD was very small, the equilibrium constant for the formation of the inclusion complex could not be evaluated using conventional capillary electrophoresis.

### *PVS-modified capillary electrophoresis of R6G*

In PVS-modified capillary electrophoresis, the electrophoretic mobility of mesityl oxide (neutral marker) was not affected by the addition of PVS, indicating no effect of PVS on the viscosity of the solution. The migration times of mesityl oxide and PVS were nearly the same, indicating no interactions between PVS and the capillary wall.

Figure 2 depicts electropherograms of R6G ($2.5 \times 10^{-4}$ M) in pH 7.5 buffers containing a fixed concentration (100

mg $L^{-1}$) of PVS and various concentrations of $\beta$-CD. With the increase in the $\beta$-CD concentration, the signal of R6G is enhanced in intensity, accompanied by the narrowing of the signal width. At $\beta$-CD concentrations below about $1 \times 10^{-2}$ M, the viscosity of the solution is little varied [15]. In addition, the electric current has not been varied irrespective of the presence of $\beta$-CD, supporting no effects on the viscosity.

As previously reported [12], the electropherogram (Figure 2a) of R6G, in which $\beta$-CD is not added, is shaped like a square wave. The square-wave type signal is due to the cooperative binding of R6G to PVS.

In a model where the binding constant of R6G towards PVS takes either a large or a small value, depending on the R6G concentration in a very small domain, into which the volume of a capillary tube is consecutively divided [12], we assume the following: (1) in each domain, the equilibrium between free R6G and R6G bound to PVS is independently established; (2) after the establishment of the equilibrium for the R6G binding in the $m$th domain, free R6G molecules in the $m$th domain move to the neighboring $(m + 1)$th domain, whereas PVS and R6G bound to PVS stay in the $m$th domain; (3) free R6G molecules in the $(m - 1)$th domain flow into the $m$th domain; (4) a new equilibrium is established for the R6G molecules existing in the $m$th domain; and (5) if free R6G molecules are absent in the $m$th domain, a new equilibrium is established for R6G, which has originally been bound to PVS in the $m$th domain. Using this scheme, we can reproduce well a square-wave type signal of R6G, which has previously been simulated [12].

To our knowledge, there is no report for the formation of an inclusion complex of PVS with CD, although CDs often form inclusion complexes with polymers [16]. Because a polymer chain of PVS is covered with strongly hydrophilic sulfonato groups, it is most likely that little or no inclusion complex is formed between PVS and CD. In addition, a ternary inclusion complex among CD, PVS, and R6G is most unlikely formed from the viewpoint of the steric factor. Consequently, CD does not seem to affect the behavior of PVS in capillary electrophoresis.

When $\beta$-CD is added to R6G solutions containing PVS, the width of the square-wave type signal becomes narrow, accompanied by the enhancement of the signal intensity, as shown in Figure 2. At high $\beta$-CD concentrations, the signal shape approaches a usually observed spike-type signal. In addition, the migration time of the rising edge of the square-wave type signal is slightly delayed. These findings are interpreted in terms of the formation of an inclusion complex between $\beta$-CD and R6G. Taking into account the dimensions of the $\beta$-CD cavity and R6G, the $\beta$-CD–R6G inclusion complex most likely has a 1:1 stoichiometry. As will be described later (Section 3.4), a spectrophotometric analysis indicates 1:1 stoichiometry for the $\beta$-CD–R6G inclusion complex. The $\beta$-CD–R6G inclusion complex is unlikely bound to PVS, because the binding site of R6G is obscured by the $\beta$-CD cavity. The formation of the $\beta$-CD–R6G inclusion complex causes the reduction in the sum of the amounts of free R6G and R6G bound to PVS in a capillary. In the PVS-modified capillary electrophoresis, where

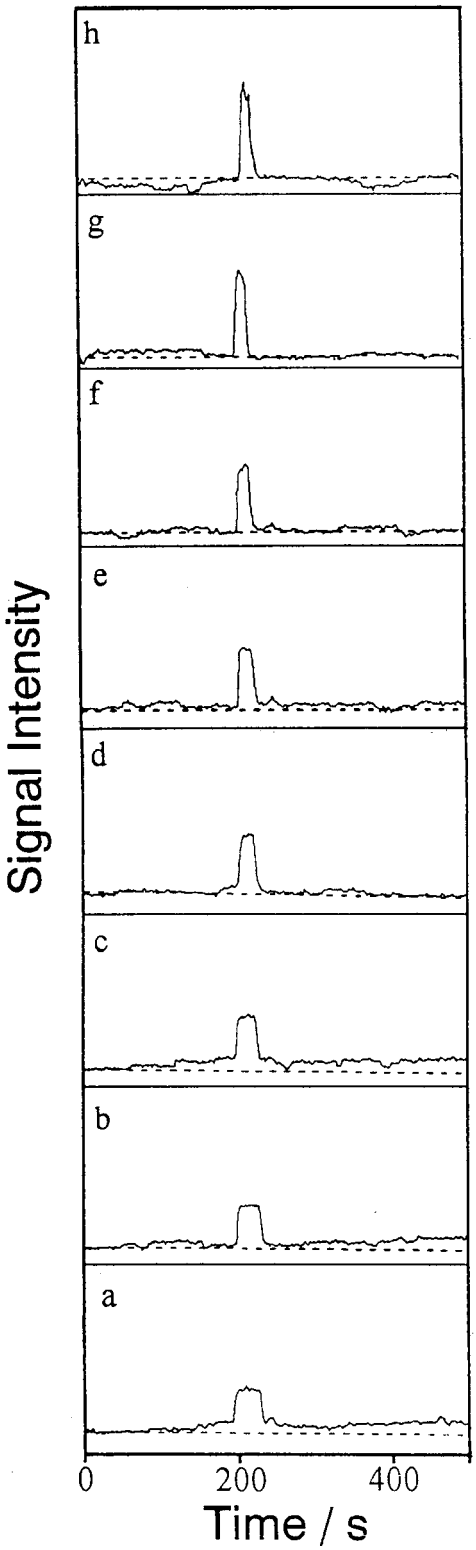


*Figure 2.* Electropherograms of R6G ($2.5 \times 10^{-4}$ M) in pH 7.5 buffers containing PVS (100 mg $L^{-1}$) and various concentrations of $\beta$-CD. Concentration of $\beta$-CD: (a) 0, (b) $1.0 \times 10^{-3}$, (c) $2.0 \times 10^{-3}$, (d) $3.0 \times 10^{-3}$, (e) $4.0 \times 10^{-3}$, (f) $5.0 \times 10^{-3}$, (g) $8.0 \times 10^{-3}$, and (h) $1.0 \times 10^{-2}$ M. The ordinate scales of the electropherograms are the same.

$\beta$-CD is not added, the concentration effects of R6G on the signal shape have already been investigated [12]; the decrease in the R6G concentration results in the decrease in the signal width of the square-wave type.

The R6G concentration is represented by the sum of the concentrations of free R6G, R6G bound to PVS, and R6G complexed with $\beta$-CD. The concentration of the $\beta$-CD–R6G inclusion complex is increased as the $\beta$-CD concentration is raised. In PVS-modified capillary electrophoresis, where $\beta$-CD is not added, the signal intensity of R6G remains constant, even if the R6G concentration is varied [12]. In a domain containing R6G, therefore, the sum of the amounts of free R6G and R6G bound to PVS is expected to be the same irrespective of the presence of $\beta$-CD; the total concentration of R6G in the domain is increased with the increase in the $\beta$-CD concentration. Consequently, the increase in the $\beta$-CD concentration leads to a decrease in the number of domains containing R6G, because the total number of R6G molecules is fixed in a capillary tube. The decrease in the number of domains containing R6G implies the decrease in the signal width of R6G.

The electrophoretic mobility of the $\beta$-CD–R6G inclusion complex is smaller than that of free, uncomplexed R6G. As a consequence, the slightly delayed migration time of the rising edge of the square-wave type signal is observed by the addition of $\beta$-CD (Figure 2).

In micellar electrokinetic chromatography, Quirino and Terabe have reported the sweeping effect, which causes the zone narrowing of an analyte, leading to a remarkable enhancement of the signal intensity (analyte concentration) [17]. In this case, however, micelle is not added to an analyte solution. In PVS-modified capillary electrophoresis, on the other hand, PVS and/or CD are introduced into both sample solution and the running buffer. Consequently, the sweeping effect is not responsible for the change in the signal shape in PVS-modified capillary electrophoresis using CD.

*Evaluation of the equilibrium constants for the formation of the inclusion complexes by means of PVS-modified capillary electrophoresis*

As previously described, the observation of the square-wave type signal (as shown in Figure 2a) can be explained by the model in which the volume inside a capillary tube is divided into very small consecutive domains. In this model, only a free R6G molecule moves to the neighboring domain under the applied electric field, whereas a R6G molecule bound to PVS does not move to the neighboring domain. In the model, the signal width of the square-wave type corresponds to the number of domains which contain R6G.

Now, we consider an injected sample of volume $v_0$, in which the R6G concentration is $[R6G]_0$. When, in each domain containing R6G near a detector, the concentrations of free R6G, R6G bound to PVS, and R6G bound to $\beta$-CD, and the volume of a domain are represented by [R6G], $[R6G]_P$, $[R6G]_{CD}$, and $v_d$, respectively, the total number of R6G molecules is equal to the number ($n$) of domains, which contain R6G, multiplied by the sum of the numbers of free R6G molecules, R6G molecules bound to PVS, and R6G molecules complexed with $\beta$-CD:

$$N_A[R6G]_0 v_0 = nN_A([R6G] + [R6G]_P + [R6G]_{CD})v_d. \quad (1)$$

Here, $N_A$ is Avogadro's number. In a domain, the equilibrium constant ($K$) for the formation of the 1:1 inclusion complex of $\beta$-CD with R6G is represented by

$$K = [R6G]_{CD}/([R6G][\beta\text{-CD}]_0), \quad (2)$$

where $[\beta\text{-CD}]_0$ is the initial concentration of $\beta$-CD. When $[R6G]_{CD}$ is less than [R6G] (the $K$ value is relatively small), the concentration of free $\beta$-CD in Equation (2) can be substituted with the initial concentration of $\beta$-CD. In the domain, the equilibrium is established between free R6G and R6G bound to PVS.

$$[R6G]_P = K'[R6G][PVS]. \quad (3)$$

Here, $K'$ is an equilibrium constant for the binding of R6G to PVS, and [PVS] is the concentration of PVS. From Equations (1)–(3), $n$ is represented as:

$$n = [R6G]_0 v_0/((1 + K'[PVS] + K[\beta\text{-CD}]_0)[R6G]v_d). \quad (4)$$

Because the signal width is proportional to $n$, one can derive an equation regarding the signal width, $w$, as a function of the $\beta$-CD concentration.

$$w = a/(1 + b + K[\beta\text{-CD}]_0), \quad (5)$$

where $a$ is the proportionality constant including a term $[R6G]_0 v_0/[R6G]v_d$, and $b$ represents $K'[PVS]$.

According to Equation (5), we have simulated the observed signal width of R6G in PVS solutions containing various concentrations of $\beta$-CD, using $a$, $b$, and $K$ as variables. The best fit least-squares simulation curve is exhibited in Figure 3, together with the observed data. From this simulation, the values of 38.3 s, 0, and 210 $M^{-1}$ are obtained for $a$, $b$, and $K$, respectively. The error in the $K$ value has been estimated to be less than 20%. The finding that the $b$ value is zero is not clear; the low concentration of PVS may be responsible for the $b$ value of 0. As an alternative explanation, the binding of R6G to PVS may be weak, because the migration time of R6G in the presence of PVS is not too delayed compared to that in the absence of PVS [12].

Figures 4 and 5 depict electropherograms of R6G ($2.5 \times 10^{-4}$ M) in pH 7.5 buffers containing a fixed concentration (100 mg $L^{-1}$) of PVS and various concentrations of $\alpha$- and $\gamma$-CD, respectively. As in the case of $\beta$-CD, the addition of $\alpha$- or $\gamma$-CD results in the narrowing of the signal width and the enhancement of the signal intensity. These findings indicate the formation of the inclusion complexes of R6G with $\alpha$- and $\gamma$-CD. From the simulation on the basis of Equation (5), the $K$ values for the formation of the 1:1 inclusion complexes with $\alpha$- and $\gamma$-CD have been evaluated to be 245 and 302 $M^{-1}$, respectively, which have estimated errors of less than 20%. Such a procedure, which evaluates the $K$ values

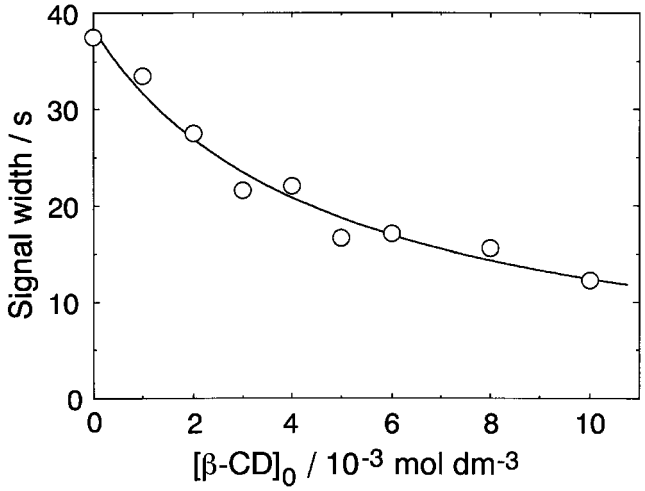


*Figure 3.* The best fit curve simulated for the signal width of R6G ($2.5 \times 10^{-4}$ M) in pH 7.5 buffers containing PVS (100 mg $L^{-1}$) and various concentrations of $\beta$-CD. The simulation curve was calculated with assumed values of $K$ = 210 $M^{-1}$, $a$ = 38.3 s, and $b$ = 0.

using PVS-modified capillary electrophoresis, may serve as a new method, when a reliable $K$ value cannot be estimated by means of conventional capillary electrophoresis.

*Evaluation of the equilibrium constants for the formation of the inclusion complexes by means of spectroscopy*

Figure 6 illustrates the absorption spectra of R6G ($1.0 \times 10^{-5}$ M) in aqueous solution containing various concentrations of $\beta$-CD. At a concentration as low as $1.0 \times 10^{-5}$ M, R6G predominantly exists as a monomer. As the $\beta$-CD concentration is increased, the absorption maximum of R6G is shifted to longer wavelengths, accompanied by an isosbestic point at 527.5 nm, although the spectral change is not too large. The absorption spectral changes are due to the formation of the $\beta$-CD–R6G inclusion complex. To compare the $K$ values obtained from the simulation of data of PVS-modified capillary electrophoresis, we have evaluated the $K$ values from the absorbance change of R6G in pH 7.5 buffers upon the addition of CDs. When a 1:1 inclusion complex is formed, the $K$ value can be evaluated from a Benesi–Hildebrand type equation [15, 18]:

$$1/(A - A_0) = 1/c + 1/(cK[\beta\text{-CD}]_0), \qquad (6)$$

where $A$, $A_0$, and $c$ are the absorbances of R6G in the presence and absence of $\beta$-CD, and a constant, respectively. Figure 7 exhibits the Benesi–Hildebrand type plot for R6G in aqueous solution containing various concentrations of $\beta$-CD. The observed wavelength was at 540 nm. The good linearity of the plot confirms the inclusional complexation with a 1:1 stoichiometry. From the plot shown in Figure 7, the $K$ value is estimated to be $330 \pm 30$ $M^{-1}$. From the absorbance change, we have similarly evaluated the $K$ values for $\alpha$- and $\gamma$-CDs to be $61 \pm 47$ and $330 \pm 40$ $M^{-1}$, respectively (not shown). As in the case of $\beta$-CD, the straight lines of the plots based on Equation (6) have supported the 1:1 stoichiometry for the complexation of R6G with $\alpha$- and $\gamma$-CDs. The $K$ values, which have been obtained from the ab-

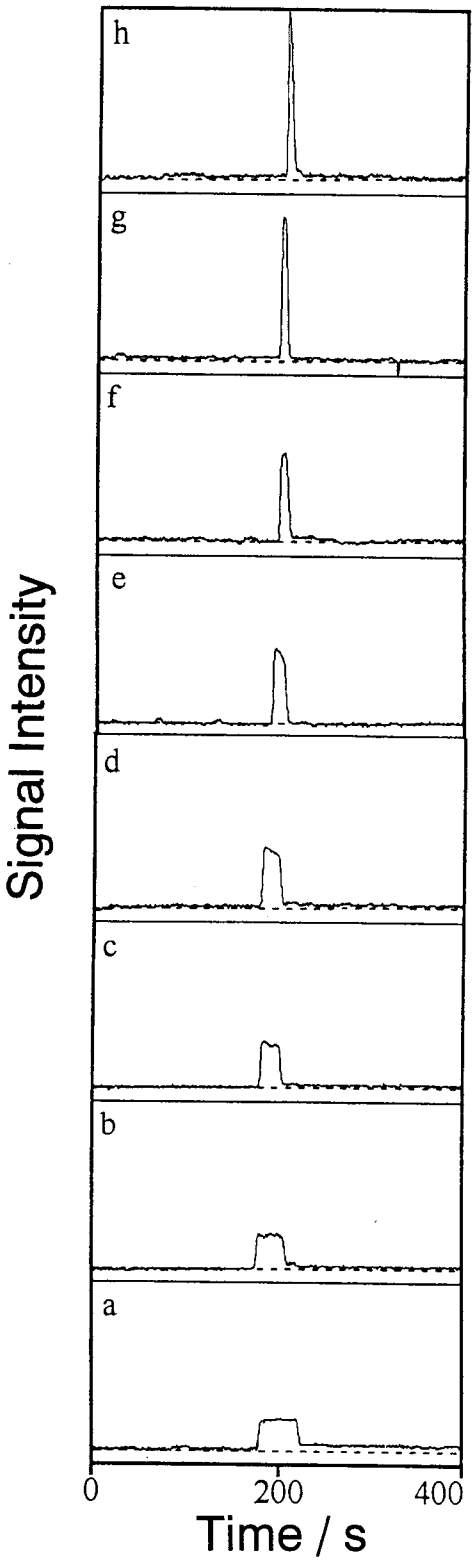


*Figure 4.* Electropherograms of R6G ($2.5 \times 10^{-4}$ M) in pH 7.5 buffers containing PVS (100 mg $L^{-1}$) and various concentrations of $\alpha$-CD. Concentration of $\alpha$-CD: (a) 0, (b) $1.0 \times 10^{-3}$, (c) $3.0 \times 10^{-3}$, (d) $5.0 \times 10^{-3}$, (e) $8.0 \times 10^{-3}$, (f) $1.0 \times 10^{-2}$, (g) $2.0 \times 10^{-2}$, and (h) $3.0 \times 10^{-2}$ M. The ordinate scales of the electropherograms are the same.

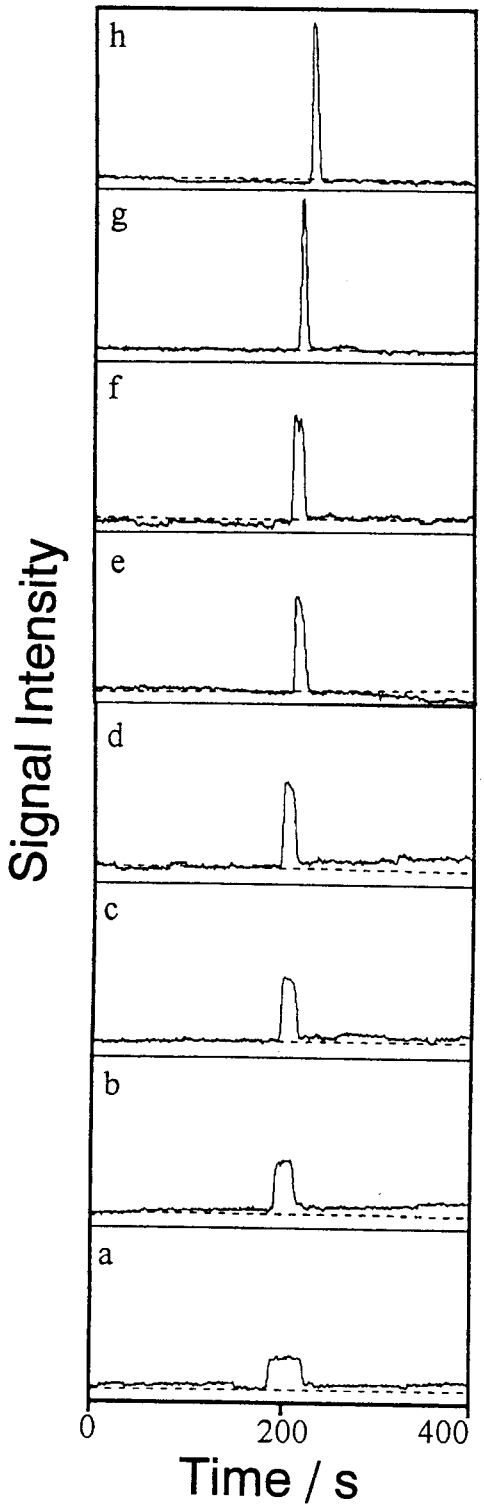


*Figure 5.* Electropherograms of R6G ($2.5 \times 10^{-4}$ M) in pH 7.5 buffers containing PVS (100 mg $L^{-1}$) and various concentrations of $\gamma$-CD. Concentration of $\gamma$-CD: (a) 0, (b) $1.0 \times 10^{-3}$, (c) $3.0 \times 10^{-3}$, (d) $5.0 \times 10^{-3}$, (e) $8.0 \times 10^{-3}$, (f) $1.0 \times 10^{-2}$, (g) $2.0 \times 10^{-2}$, and (h) $3.0 \times 10^{-2}$ M. The ordinate scales of the electropherograms are the same.

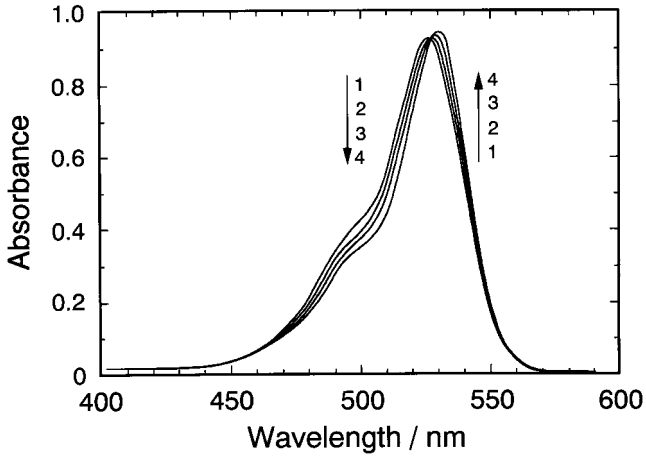


*Figure 6.* Absorption spectra of R6G ($1.0 \times 10^{-5}$ M) in pH 7.5 buffers containing various concentrations of $\beta$-CD. Concentration of $\beta$-CD: (1) 0, (2) $1.0 \times 10^{-3}$, (3) $3.0 \times 10^{-3}$, and (4) $1.0 \times 10^{-2}$ M.

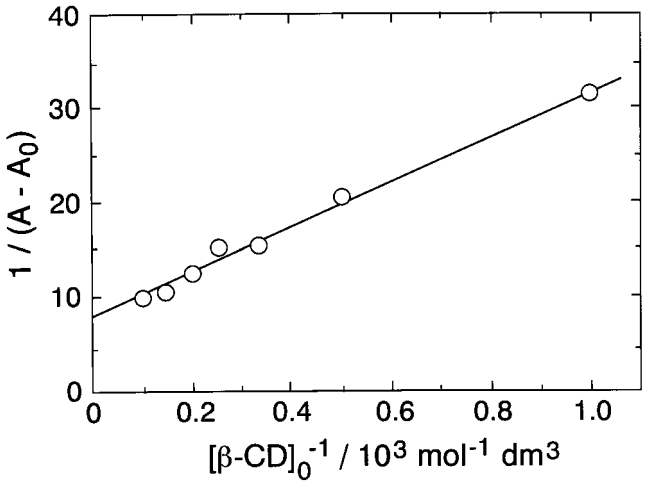


*Figure 7.* Benesi–Hildebrand type plot for R6G ($1.0 \times 10^{-5}$ M) in pH 7.5 buffers containing various concentrations of $\beta$-CD. $\lambda_{obs} = 540$ nm.

sorbance change, for $\beta$-and $\gamma$-CDs are comparable to those evaluated from PVS-modified capillary electrophoresis. In the case of $\alpha$-CD, however, the $K$ value evaluated from the spectrophotometric method is one-fourth of that evaluated from PVS-modified capillary electrophoresis. In capillary electrophoresis, the dimerization of R6G may occur to some extent, because the concentration of R6G is higher than that used in spectrophotometry. In PVS-modified capillary electrophoresis, however, the concentration of free R6G in each domain is unlikely to be high, because R6G distributes over the wide range of the domains. At present, it is not clear why the $K$ values evaluated for $\alpha$-CD from the two methods are different from each other.

From induced circular dichroism spectral changes, the $K$ values of fluorescein, which is a xanthene dye, have been reported to be $35 \pm 10$, $360 \pm 40$, and $35 \pm 10$ $M^{-1}$ for $\alpha$-, $\beta$-, and $\gamma$-CD, respectively, [19]. With respect to $\beta$-CD, the $K$ value of R6G is close to that of fluorescein, although the $K$ values of R6G for $\alpha$- and $\gamma$-CDs are respectively greater than those of fluorescein. For erythrosine B, the $K$ values of $20 \pm 10$, $40 \pm 20$, and $110 \pm 20$ $M^{-1}$ have also been evaluated for $\alpha$-, $\beta$-, and $\gamma$-CD, respectively. On the other hand, the $K$

value of rhodamine B for $\beta$-CD has been estimated to be 2900 $M^{-1}$ [20].

## Conclusions

In conventional capillary electrophoresis, the addition of CD resulted in a very slight delay of the migration time of R6G. Consequently, the $K$ value for the formation of the inclusion complex of R6G with CDs could not be evaluated using conventional capillary electrophoresis. When PVS is added to sample solutions and running buffers, the signal shape of R6G in capillary electrophoresis is changed to a square-wave type. In the PVS-modified capillary electrophoresis, the intensity and width of the square-wave type signal of R6G is enhanced and narrowed, respectively, upon the addition of $\alpha$-, $\beta$-, or $\gamma$-CDs. In addition, the migration time of the rising edge of the square-wave type signal is very slightly delayed by the addition of CD. The formation of the inclusion complexes of R6G with CDs is responsible for the variation of the intensity, width, and migration time of the R6G signal with the CD concentration. From the simulations of the changes in signal width upon the addition of CD, the $K$ values for the formation of the 1:1 inclusion complexes of R6G with $\alpha$-, $\beta$-, and $\gamma$-CDs have been evaluated to be 245, 210, and 302 $M^{-1}$, respectively. The $K$ values for $\beta$- and $\gamma$-CDs are comparable to those obtained from the absorbance changes in spectrophotometry, although the $K$ value for $\alpha$-CD is about four times greater than that obtained from the absorbance change.

## References


1. W. Saenger: *Angew. Chem. Int. Ed. Engl.* **19**, 344 (1980).
2. S. Fanali: *J. Chromatogr. A* **875**, 89 (2000).
3. A.M. Stalcup and K.H. Gahm: *Anal. Chem.* **68**, 1360 (1996).
4. D.W. Armstrong, L.W. Chang, and S.S.C. Chang: *J. Chromatogr. A* **793**, 115 (1998).
5. W. Zhu, F. Wu, F.M. Raushel, and G. Vigh: *J. Chromatogr. A* **895**, 247 (2000).
6. D.M. Davies and M.E. Deary: *J. Chem. Soc., Perkin Trans. 2* 2423 (1996).
7. C.N. Sanrame, R.H. de Rossi, and G.A. Arguello: *J. Phys. Chem.* **100**, 8151 (1996).
8. S. Hamai and H. Sakurai: *J. Chromatogr. A* **800**, 327 (1998); S. Hamai and H. Sakurai: *Anal. Chim. Acta* **402**, 53 (1999).
9. S. Hamai: *J. Phys. Chem. B* **101**, 1707 (1997).
10. S. Hamai: *J. Phys. Chem. B* **103**, 293 (1999).
11. O.S. Tee, S.M.I. Hussein, I.E. Turner, and O.J. Yazbeck: *Can. J. Chem.* **78**, 436 (2000).
12. S. Hamai and K. Sasaki: *Microchem. J.* **69**, 27 (2001).
13. K.L. Rundlett and D.W. Armstrong: *J. Chromatogr. A* **721**, 173 (1996).
14. B.A. Williams and G. Vigh: *Anal. Chem.* **68**, 1174 (1996).
15. S. Hamai: *Bull. Chem. Soc. Jpn.* **55**, 2721 (1982).
16. A. Harada: *Coordinat. Chem. Rev.* **148**, 115 (1996).
17. J.P. Quirino and S. Terabe: *Anal. Chem.* **71**, 1638 (1999).
18. H.A. Benesi and J.H. Hildebrand: *J. Am. Chem. Soc.* **71**, 2703 (1949).
19. L. Flamigni: *J. Phys. Chem.* **97**, 9566 (1993).
20. Y. Degani, I. Willner, and Y. Haas: *Chem. Phys. Lett.* **104**, 496 (1984).